Monitoring of Progressive Microcracking in Concrete Using Diffuse Ultrasound

P. SHOKOUHI

ABSTRACT

Diffuse ultrasonic measurements are used to monitor progressive stress-induced damage (microcracking) in a concrete specimen. The specimen was subjected to stepwise uniaxial compression. At each step, the loading was held constant and a series of ultrasonic measurements parallel and perpendicular to the loading were obtained. Unusually long signals were recorded, so that the diffuse ultrasonic regime could be studied. Using Coda Wave Interferometry (CWI), the corresponding changes in the velocity of diffuse ultrasonic waves and the evolution of non-linear material parameter were monitored. The changes were observed to highly relate to the state of volumetric microcracking at various load levels.

INTRODUCTION

The ultrasonic pulse velocity (UPV) method has long been used for concrete evaluation. The measurement setup consists of a pair of ultrasonic transducers acting as sender and receiver. The velocity is obtained by measuring the time-of-flight (TOF) of the transmitted pulse over a known distance within the material. The stress-dependency of UPV in concrete has been investigated in a number of studies, where a decrease in ultrasonic pulse velocities in concrete at stress levels higher than 70% of the strength has been reported [*1-4*]. Suaris et al. [*3*] showed that the amplitude of the ultrasonic waves begins to decrease when the stress reaches to about 40% of the strength, concluding that the amplitude is more sensitive to the state of damage than the velocity. This observation was later confirmed by Nogueira and Willam [*4*].

The effects of stress-induced damage in concrete on ultrasonic measurements were investigated here. However, instead of the coherent field (i.e. the early part of the signal), the diffuse field (i.e. the later part or Coda) of ultrasonic signals was analyzed.

Parisa Shokouhi, Dept. 8, BAM - Federal Institute for Material Research and Testing, Unter den Eichen 87, D-12205, Berlin, Germany

Coda waves constitute the trail of strongly scattered waves in an ultrasonic signal (***Figure 1***). Coda waves are sensitive to changes in the medium because the scattering that generates these waves causes coda waves to repeatedly sample a limited portion of the material. Coda wave interferometry (CWI) is a technique that exploits this sensitivity to estimate weak changes in the medium from a comparison of the coda waves before and after the perturbation [*5*]. This method was developed by seismologists over 20 years ago, mainly to detect slight velocity changes in the earth crust due to seismic effects, mining influence or seasonal variations [*5-7*]. It was not until very recently that CWI was used to detect small changes in concrete microstructure (e.g. *8*, *9*).

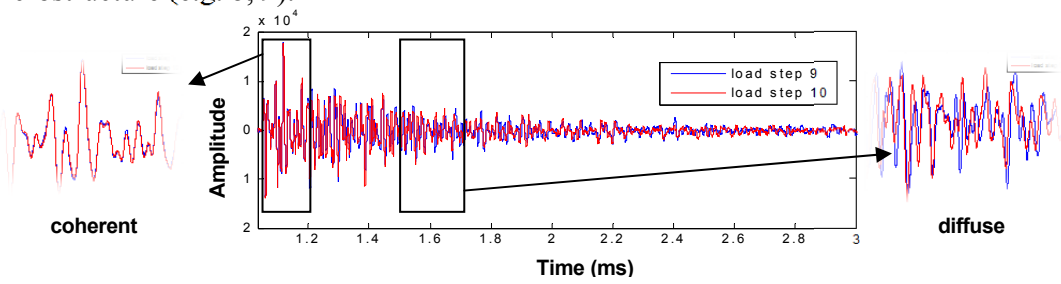

Figure 1. Coherent and Incoherent (diffuse) ultrasonic fields.

CODA WAVE INTERFEROMETRY (CWI)

The CWI algorithm utilized [*6*, *8*] is based on the assumption that, the perturbation causes the waveforms to be stretched (or compressed) in time. To obtain the velocity change ($v = dV/V$), the perturbed signal h_j should be first interpolated at times $t(1-v)$ with various velocity changes v. The desired velocity change v^* is the v that maximizes the cross-correlation coefficient between the perturbed signal $h_j\,(t(1-v))$ and the reference signal $h_0(t)$ calculated in the selected time window $[t_0\ T]$. The main advantage of this approach is the increased accuracy in measuring travel tiem changes, which are not possible to detect using the conventional TOF approach. The chart in ***Figure 2*** illustrates the calculation steps in the form of a flow-chart diagram.

EXPERIMENTAL STUDY

The stress-dependency of coherent and diffuse ultrasonic wave velocities in concrete was investigated in several experiments, two of which will be discussed in this paper. The details of the test specimen, equipment and the measurement procedure are given in this section.

Test Specimen

Prismatic plain concrete specimens of size 0.2 x 0.2 x 0.6 m^3 (7 7/8 x 7 7/8 x 23 5/8 $in.^3$) were tested in the experiments discussed in this paper. The concrete mix was prepared according to the C30/C37 mix design given in the European (Eurocode2) or German guidelines (DIN 1045-1) with a maximum aggregate size of 16 mm and water-cement ratio of 0.55. Five identical specimens of the same batch were cast in wooden molds. The specimens were stripped of the molds after 5 days and then put in ambient conditions for at least 28 days before being tested.

$$CC_j(v) = \frac{\int_{t_0}^{T} h_j(t(1-v))h_0(t)dt}{\sqrt{\int_{t_0}^{T} h_j^{\,2}(t(1-v))dt \int_{t_0}^{T} h_0^{\,2}(t)dt}}$$

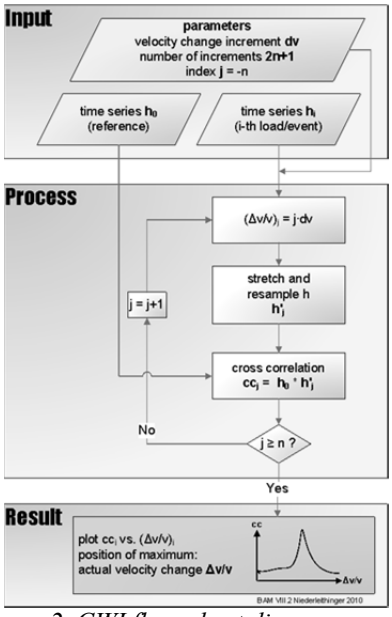

Figure 2. CWI flow-chart diagram.

Testing Apparatus

Identical testing equipment was used in both experiments. The test equipment consisted of a 20 MN-loading machine and the instrumentation necessary for ultrasonic and deformation measurements. As shown schematically in **Figure 3**, ultrasonic measurements were taken in transmission mode and along two perpendicular directions (i.e. parallel and perpendicular to the loading). A pair of 100-KHz longitudinal ultrasonic sensors from Acsys (Acoustic Control Systems Ltd.) was used for measurements in either direction. The ultrasonic sensors were all of dry point contact type and their application did not require the use of any coupling agents. The two sensors used for the measurements parallel to the loading were built in the loading plates, while the other two (for ultrasonic measurements perpendicular to the loading) were mounted on the surface of the specimen. An in-house built frame and two holders were used to attach the sensors to the surface of the specimen and to ensure that they remain in full contact over the entire duration of the test.

The deformation of the specimen under the load was recorded in both directions using linear variable displacement transducers (LVDTs). As depicted in ***Figure 3(b)***, four LVDTs were installed in either direction. A number of strain gauges (not shown in ***Figure 3***) were also used for 'backup' deformation measurements.

Test procedures

The specimen was instrumented and then placed in the loading machine, exactly in the middle of the loading plates. The specimen was then gradually loaded along its length in prescribed load/strain steps (stress/strain-controlled). In the first experiment, the specimen was subjected to only one cycle of loading; the load was applied in a stress-controlled manner, in steps of 50 KN or 1.25 MPa. The stepwise loading continued until the specimen broke at 1250 KN or 31.25 MPa (stress-strength ratio of 100%). In the second experiment, the specimen was subjected to six subsequent

loading-unloading cycles of maximum stress-strength ratios of 10%, 38%, 68%, 39%, 76% and 100%, respectively. The loading was applied and removed in a strain-controlled manner. The experiment was completed in two successive days; cycles 1 to 3 were completed in Day 1 and cycles 4 to 6 were completed during Day 2.

In both experiments, the very first set of ultrasonic measurements was taken before the loading began, at the stress-free (or zero-load) state. At every subsequent load step, the deformation (and not the load) was held constant long enough to allow taking all the measurements. The measurements along each direction were repeated ten (10) times. Therefore, a total of twenty (20) ultrasonic signals per load step were recorded. Once the measurements were completed, the load/strain was increased to the next prescribed level. This procedure continued until the specimen broke (in the first experiment) or the maximum desired load level in the corresponding load cycle was achieved (in the second experiment). Although the instruments were not dismounted at the final stages of loading (close to the failure), fortunately, no damages were encountered.

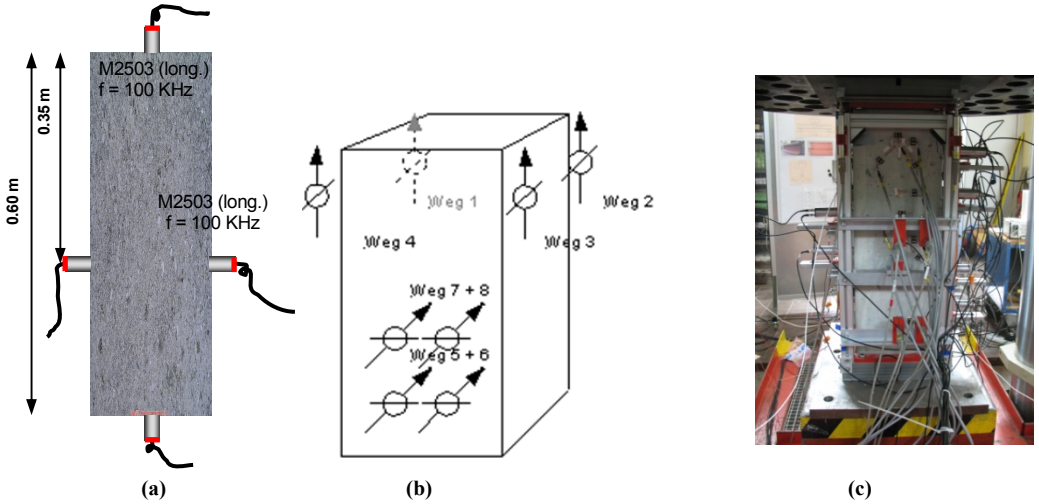

Figure 3. Schematics of the experimental setup for (a) ultrasonic and (b) deformation measurements. The instrumented specimen under load is shown in (c).

EXPERIMENTAL RESULTS

First, the changes in the corresponding TOF velocities with the gradually increasing stress were calculated. The TOF velocities were then corrected for the specimen longitudinal and lateral deformations. As seen in ***Figure 4***, the TOF velocities do not show great sensitivity to the level of stress in concrete over the early load steps (low stress levels). It is not until reaching the critical levels that the changes in TOF velocities become notable. The observed trend of velocity changes agrees very well with those reported previously by other researchers [e.g. *4*].

The CWI velocities, superimposed on TOF velocities, are also shown in ***Figure 4.*** A slightly different approach has been taken in calculating the CWI velocities here. Since the load step size (1.25 MPa) was considerably large in this experiment, the correlation coefficient *CC* calculated between the record at the stress-free state and the records obtained at later load steps, soon deviated from the ideal unity. After a few (about 10) load steps, it was even hardly possible to detect a reliable peak in the *CC* vs. *v* curve (see ***Figure 2***) and deduce the velocity change. Therefore, instead of using

the first record as the reference signal, the correlation coefficient CC was calculated incrementally between the pair of signals recorded at two subsequent load steps. The accumulated errors were calculated and proved to be insignificant, as reflected in the very small size (hardly seen) of the error bars depicted in ***Figure 4***.

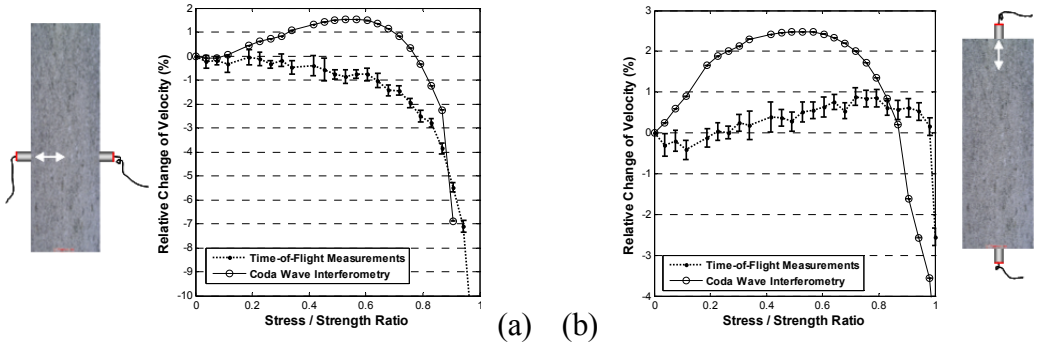

Figure 4. Relative stress-induced velocity changes obtained using TOF and CWI in two directions: (a) parallel and (b) perpendicular to the load.

The CWI velocities obtained during the second experiment are shown in ***Figure 5***. The velocities (corrected for the specimen deformation) are plotted against the load step numbers. The maximum load level in each cycle is marked with the corresponding maximum stress-strength ratio in %. The velocity increases monotonically during the first, second and fourth cycles, because the maximum load levels for these cycles are low, 10%, 38% and 39%, respectively. The velocity-stress trends in the third, fifth and last cycles however closely follow the trend measured earlier in the first experiment. Similar to what was reported earlier for the first experiment, the velocity changes are greater, when measured parallel to the loading.

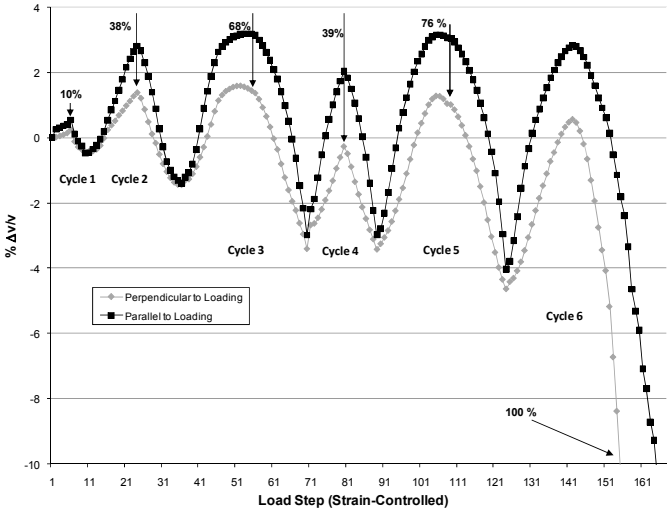

Figure 5. Relative CWI velocity changes measured parallel and perpendicular to the loading in the second experiment.

5.2 Effect of Damage on the Velocity-Stress Relationship

Stress-dependency of ultrasonic wave velocities in metals is typically explained based on acoustoelastic theory [*12-14*]. The first order approximation of this theory predicts a linear relationship between the relative change in velocity and strain for

non-linear elastic materials. The longitudinal wave velocities in a uniaxially-loaded column of nonlinear elastic constituents (as shown in ***Figure 6***) change according to:

$$\frac{\Delta V_{11}^{\sigma_1}}{V_{11}^0} = -\varepsilon_{11}\beta_{11} \quad \frac{\Delta V_{22}^{\sigma_1}}{V_{22}^0} = -\varepsilon_{11}\beta_{22}$$

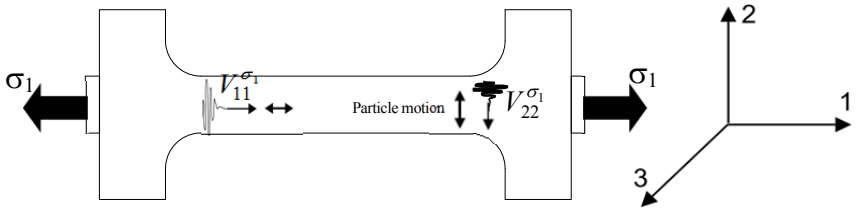

Figure 6. Acoustoelasticity predicts a linear relationship between the relative changes of ultrasonic wave velocities with strain.

Where V_{11} and V_{22} are ultrasonic (longitudinal) wave velocities measured along axes 1 and 2, ε_{11} is the elastic strain and β is the proportionality coefficient known as the non-linear parameter β. This parameter is a combination of Lame's constants and the 3rd order elastic constants. Given that CW velocities are a weighted average of longitudinal and transverse wave velocities and the specimen was under compression, the equations above were modified as follows:

$$\frac{\Delta\Sigma\alpha_{ij}V_{ij}}{V_P} = \varepsilon_{11}(\beta_{11}^*) \quad \frac{\Delta\Sigma\alpha_{ij}V_{ij}}{V_P} = \varepsilon_{11}(\beta_{22}^*)$$

where the asterisk * is used to distinguish the proportionality coefficient applicable to CWI velocities; β^* is the slope of the relative change of CWI velocity curve versus strain measured over the elastic (reversible) region. β_{11}^* and β_{22}^* refer to the CWI velocity- strain slopes measured parallel and perpendicular to the loading, respectively. These two parameters were estimated over the elastic strain range (i.e., $\varepsilon < 0.1\%$). In calculation of these parameters, the very first point was excluded.

The evolution of β_{11}^* and β_{22}^* with the increasing level of damage caused by the load application over cycles 1 to 5 is shown in ***Figure 7*** below. It should be noted that β^* is calculated over the elastic range at the beginning of each new cycle, when the loading is too low to initiate considerable new damage (microcracking) in the specimen. Therefore, in this figure, β^* calculated for Cycle *n* is related to the maximum stress-strength ratio of the previous cycle, Cycle *n-1*.

The non-linear parameter β^* increases rapidly with the increasing stress-strength ratios of up to about 40 %, after which the rate of increase of β^* significantly drops. In another words, β^* seem to be more sensitive to the slight changes in concrete microstructure. From microscopic point of view, the stress-induced increase in the velocity of concrete is a result of the closure of microcracks [*16*]. The more microcracks are closed, the higher is the expected increase in the measured velocities and consequently, β^* measures higher. However, after reaching certain stress-strength levels, the microcracks are widened and may no longer be close under the application of the first few load steps in the elastic region. After reaching this stage, the increase rate of β^* slows down. For all the load cycles, β_{11}^* is greater than β_{22}^*.

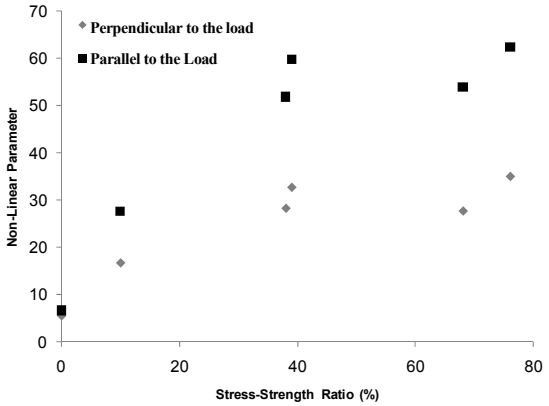

Figure 7. The evolution of the non-linear parameter β^* with the increasing level of stress over Cycles 1 to 5.

DISCUSSION AND CONCLUSIONS

CWI and TOF velocities are not immediately comparable. A diffuse field in a homogeneous solid medium partitions its energy between transverse and longitudinal waves in a ratio $R = 2(V_P/V_S)^3$, where V_P and V_S denote the compression and shear wave velocities of the medium [*11*]. Although the heterogeneity of concrete makes the diffusive energy partitioning even more complicated. Therefore, the CWI velocity is a weighted average of longitudinal and transverse velocities $\Sigma\alpha_{ij}V_{ij}$ (as well as the surface waves travelling around the specimen), even though longitudinal transducers were used. The TOF velocities are on the other hand, the longitudinal ultrasonic velocities measured along two perpendicular directions. Nevertheless, the CWI velocities show much greater sensitivities to the subtle stress-induced changes in the microstructure of concrete.

Not only are the velocity changes greater, but also show particular characteristics, which are useful in structural health monitoring (SHM) applications. The CWI velocities measured in both directions attain maxima at a stress-strength ratio of about 55%, well before the specimen reaches the critical levels of stress. Afterwards, the velocities start to gradually decrease. The velocities drop significantly after the stress/strength ratio goes beyond 80%. Therefore, such measurements can be used for monitoring in the warning mode. Moreover, the velocity changes are direction dependent; the changes in velocities measured parallel to the loading are greater than those measured perpendicular. Velocity-stress relationships were reduced to obtain a modified non-linear index parameter β^*. This parameter exhibits high sensitivity to early microcracking. Measuring the nonlinear material parameters, damage processes can be monitored, which result in subtle changes in concrete microstructure and typically go undetected by conventional test methods.

REFERENCES

1. N. K. Raju (1970), Small Concrete Specimens under Repeated Compressive Loads by Pulse Velocity Technique, Journal of Materials, Vol. 5, No. 2, pp. 262-273.

2. S. P. Shah and S. Chandra (1970), Mechanical Behavior of Concrete Examined by Ultrason- ic Measurements, Journal of Materials, Vol. 5, No. 3, pp. 550-563.
3. W. Suaris and V. Fernando (1987), Detection of Crack Growth in Concrete from Ultrasonic Intensity Measurements, Materials and Structures, Vol. 20, pp. 214-220.
4. C. L. Nogueira and K. J. Willam, (2001), Ultrasonic Testing of Damage in Concrete under Uniaxial Compression, ACI Materials Journal, 98, 3, 265-275.
5. R. Snieder, A. Grêt, A., H. Douma, and J. Scales (2002), Coda Wave Interferometry for Es- timating Nonlinear Behavior in Seismic Velocity, Science, 295, 253–2255.
6. C. Sens-Schönfelder and U. Wegler (2006), Passive Image Interferometry and seasonal variations of seismic velocities at Merapi volcano, Indonesia, Geophysics Research Letters, 33, L21302.
7. A. Grêt, R. Snieder, R., and U. Özbay (2006), Monitoring in situ stress changes in a mining environment with coda wave interferometry, International Journal of Geophysics, 167, 504– 508.
8. E. Larose and S. Hall (2009), Monitoring stress related velocity variation in concrete with a 2.10-5 relative resolution using diffuse ultrasound, Journal of Acoustical Society of America, 125, 4, 1853-1856.
9. S. Stähler, E., Niederleithinger, S., Pirskawetz, T.-R., Nowak, and F. Weise (2009), Detect- ing subtle changes in materials by coda wave interferometry. In Sens-Schönfelder, C., Ritter, J., Wegler, U.,and Große, C.,editors, Noise and Diffuse Wavefields – Extended Abstracts of the Neustadt Meeting, pages 59–62. Deutsche Geophysikalische Gesellschaft.
10. A. Zoëga, P. Shokouhi, and H. Wiggenhauser (2009), Propagation Time of Elastic Surface Waves on Concrete Specimens under Uniaxial Loads, Journal of Structural Engineering, 36, 1, 11-15.
11. R. L. Weaver (1982), On Diffuse Waves in Solid Media, Journal of the Acoustical Society of America, 71, 6, 1608-1609.
12. D. S. Hughes and J. L. Kelly (1953), Second-Order Elastic Deformation of Solids, Physical Review, V. 92, No. 5, pp. 1145-1149.
13. S. Takahashi, S. and R. Motegi, R. (1987), Stress Dependency on Ultrasonic Wave Propagation Velocity – Part I: Analysis by the Eulerian Viewpoint of Ultrasonic Wave Velocity in the Uniformly Deformed Isotropic Solid, Journal of Materials Science, V. 22, pp. 1850- 1856.
14. R. M. Bergman and R. A. Shahbender (1958), Effects of Statically Applied Stresses on the Velocity of Propagation of Ultrasonic Waves, Journal of Applied Physics, V. 29, pp. 1736- 1738.
15. V. Hauk (1997), Structural and Residual Stress Analysis by Nondestructive Methods: Evaluation – Application – Assessment, Elsevier Science B.V., Amsterdam, The Netherlands.
16. P. Shokouhi, A. Zoëga, H. Wiggenhauser and G. Fischer (2012), Surface Wave Velocity - Stress Realtionship in Uniaxially Load Concrete, ACI Journal of Materials, 109(2), pp. 131-139.